sciendo

Int. J. of Applied Mechanics and Engineering, 2021, vol.26, No.2, pp.173-185
DOI: 10.2478/ijame-2021-0026

A NUMERICAL APPROACH TO SLIP FLOW OF A MICROPOLAR FLUID ABOVE A FLAT PERMEABLE CONTRACTING SURFACE

R. PARTHIBAN
Department of Mathematics, Government Arts College for Men
Affiliated to University of Madras, Chennai, INDIA

G. PALANI*
Department of Mathematics, Dr. Ambedkar Govt. Arts College
Affiliated to University of Madras, Chennai, INDIA
E-mail: gpalani32@yahoo.co.in

Seema TINKER
Department of Mathematics, JECRC University Jaipur-302033, INDIA

R. P. SHARMA
Department of Mechanical Engineering, National Institute of Technology
Arunachal Pradesh-791112, INDIA

A plain linear penetrable contracting sheet with slip over a micro-polar liquid with a stagnation-point flow is analyzed. Through similarity mapping, the mathematical modeling statements are transformed as ODE's and numerical results are found by shooting techniques. The varying impacts of physical quantities on the momentum, micro-rotation, and temperature were demonstrated through graphs. The computed measures including shear and couple stress with distinct measures of factors involved in this proposed problem are presented through a table.

Key words: boundary layers, heat sink, micro-polar fluid, slip condition, and suction or injection.

1. Introduction

Heat transmission past a stretching surface has a lot of manufacturing applications which include optical filament manufacture, hot involution cable graphics, the aerodynamic expulsion of elastic foils, metal spinning, and pulling elastic foils. Miklavcic and Wang [1] examined the viscid flow prompted by a contracting surface. The closed-form solutions were obtained. Wang [2] analyzed a stagnation point flow over a contracting surface and obtained that the heat exchange rate declines with the contracting rate because of the growth in the boundary layer thickness. Nadeem *et al.* [3] considered second quality liquid with the contracting surface and discussed axisymmetric and 2-dimensional shrinking flow. Bachok *et al.* [4] carried out an analysis to examine heat transfer and 2-D stagnation-point flow, a laminar liquid movement to an expanding/contracting surface. The pertaining equations were solved and the impact of various factors involved in the problem was analyzed. Fan *et al.* [5] studied the flow along a contracting surface and high accurate analytical approximations well agreed with the results provided by the Keller-Box scheme. In a porous medium, heat transfer, as well as stable stagnation flow along a contracting surface, was examined by Rosali *et al.* [6]. Heat transfer as well as flow behaviour for numerous values of the parameter involved into the problem, were analyzed and outcomes

* To whom correspondence should be addressed

pointed out the dual solutions for the contracting case. Bhattacharyya and Vajravelu [7] analyzed heat transfer stagnation flow towards an exponential contraction sheet. The investigation disclosed that if velocity ratio factors fulfill inequality $-1.487068 \le c/a$, then the solution will exist. Bachok *et al.* [8] examined a 2-D stagnation flow of a nano-liquid along a contracting/elongating surface. The solution achieved solely depends upon the parameters taken into an account.

In the Newtonian and non-Newtonian flow theory, heat transfer and flow performance of particular fluids, namely polymeric fluids, paints, colloidal fluids, liquid crystals, lubricating oils and animal blood cannot be described. These types of fluids have many governing equations that do not operate according to Newton's law. To overwcome such a complication, Eringen [9] developed the concept of micro fluids, which handles types of fluids showing particular microscopic impacts rising from the shape along with micro-movements of liquid components. These liquids support the stress moment and are affected by the spiral recession. Later Eringen [9] created a subcategory of these fluids, called micro-polar fluid, in which micro-rotation effects and micro rotation inertia exist, but do not to support stretch. It can support body couples as couple stress.

Kumari and Nath [10] considered a 2-dimensional unstable axisymmetric body flow of micropolar liquids. Heat transfer is affected considerably by the Prandtl number and time-dependent varying wall temperature, whereas the micro-rotation gradient and shearing stress are unaffected by them. Zial Haque *et al.* [11] discussed the behavior of an MHD micropolar liquid in a porous medium. Nachtsheim – Swigert repletion procedure was engaged as the main device to find the numerical solution. Through graphs, the influences of the numerous important factors on velocity, angular velocity, temperature as well as species contours were discussed in detail. The impact of the ruling factors on shear stress was explained in the tables.

Uddin and Kumar [12] analyzed the impact of Hall current and MHD flow of micropolar liquid over non-conducting wedge along with ion-slip and proposed to solve the ruling equations approximately. The influence of numerous factors considered in the study have was analyzed with the assistance of graphs, values of the Nusselt number and shearing stress were offered in a tabular form and a comparative study was also made. The 3-D flow of a micropolar liquid on stiff uncharged dielectric at rest was examined by Borrelli *et al.* [13]. The impact of the ruling factors on the magnetic field and liquid flow was exhibited graphically and discussed. Siva and Shamshuddin [14] considered a chemically reactive and viscous dissipative flow of a micro-polar liquid along a plumb holey moving surface implanted in a leaky medium. A set of ordinary differential equations (non-linear) was derived from partial differential equations and then numerical values were obtained by using the finite element procedure.

The studies of micropolar fluids over a stretching surface are important from the technological point of view because they have many uses in chemical and metallurgy engineering. Rahman *et al.* [15] examined a 2-D MHD flow of a micropolar liquid along a non-linear contracting surface without uniform wall temperature and varying viscosity. The similarity solutions were acquired by using the Nachtsheim-Swigert repetition process. They have a non-linear contracting and temperature index that depends on the heat exchange rate. Ishak *et al.* [16] examined the 2-D flow of a micro-polar liquid along with a contracting sheet. Yacob *et al.* [17] investigated a micro-polar liquid flow over a horizontal linear elongating/contracting sheet with stagnation. A mathematical model for elongating/contracting sheet is established to analyze the heat transfer during the melting process.

Bhattacharyya *et al.* [18] studied radiative effects of a micro-polar liquid flow over a porous contracting surface. The similarity mappings were used to convert PDEs to ODE's and approximate solutions were achieved by using a shooting method. Hussain *et al.* [19] presented radiative effects on the unstable micropolar liquid flow along a stretching surface. A non-dimensional form of the flow problem was achieved by using similarity variables for a permeable sheet. The homotopy analysis method is engaged to get the solutions for various flow parameters. The impacts of a chemically reactive on MHD micropolar liquid stagnation flow through a contracting sheet were studied by Khilap Singh *et al.* [20].

This type of flow has wide applications from chemical engineering to geophysics. Working fluid with heat source/sink effects plays a vital role in certain porous media applications. Subhas Abel *et al.* [21] illustrated liquid flow towards a linearly contracting surface with varying heat source/sink and the Keller Box technique was engaged to find the solution. Mahmoud and Waheed [22] discussed impacts of a slip

velocity flow on an MHD micro-polar fluid with heat generation along with a permeable contracting sheet. Numerical solutions were achieved by using the Chebyshev spectral method. Slip factor impacts on angular velocity as well as temperature contours were discussed in detail with graphs.

Mabood *et al.* [23] investigated a 2-D magneto hydro-dynamic micro-polar liquid movement along a contracting surface inserted in a porous medium. Numerical results were compared with the earlier results and were found to be in excellent agreement. Muthamilselvan *et al.* [24] studied numerically a free convective micro-polar liquid in a square pit with the hot tinny plate and the solutions were obtained by a finite volume method. The impact of different values of the Prandtl number, Rayleigh number, heat source, vortex viscosity factor, and source factors on the fluid flow was analysed. Due to the occurrence of the vortex viscosity factor, fluid velocity was observed to be slow. Mishra *et al.* [25] analysed a micropolar liquid stream above a flat plate with a radiative heat source.

Motivated by the above works, the authors have analysed a micropolar fluid flow about a contracting surface with stagnation-point. Through similarity mapping the modeling mathematical statements are transformed to joined ODEs and using MATLAB software, quantitative outcomes are found by employing the shooting method with the Runge-Kutta method.

2. Formation of equations

A 2-D stagnation-point micropolar liquid flow above a flat linear penetrable shrinking surface with slip conditions is considered. The coordinate system of the flow is explained in Fig.1. It is assumed that the velocity near the surface and velocity of the external flow is $\bar{u}_w(\bar{x}) = a\bar{x}$ and $\bar{u}_e(\bar{x}) = c\bar{x}$, respectively, here $a > 0, c > 0$. The $\bar{x}$-axis is taken along the sheet. The impacts of microstructure, viscous dispersion as well as radiation are presumed to be naught and the total spin $\bar{N}$ of the micro rotation is reduced.

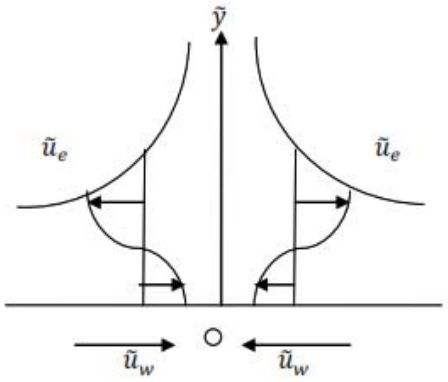

Fig.1. Flow model.

The continuity, velocity, micro-rotation as well as energy equations are as follows:

$$\frac{\partial \bar{u}}{\partial \bar{x}} + \frac{\partial \bar{v}}{\partial \bar{y}} = 0, \tag{2.1}$$

$$\bar{u}\frac{\partial \bar{u}}{\partial \bar{x}} + \bar{v}\frac{\partial \bar{u}}{\partial \bar{y}} = \bar{u}_e\frac{\partial \bar{u}_e}{\partial \bar{x}} + \left[\frac{\mu + \kappa}{\rho}\right]\frac{\partial^2 \bar{u}}{\partial \bar{y}^2} + \left[\frac{\kappa}{\rho}\right]\frac{\partial \bar{N}}{\partial \bar{x}}, \tag{2.2}$$

$$\rho j\left[\bar{u}\frac{\partial \bar{N}}{\partial \bar{x}} + \bar{v}\frac{\partial \bar{N}}{\partial \bar{y}}\right] = \gamma\frac{\partial^2 \bar{N}}{\partial \bar{y}^2} - \kappa\left[2\bar{N} + \frac{\partial \bar{u}}{\partial \bar{y}}\right], \tag{2.3}$$

$$\bar{u}\frac{\partial \bar{T}}{\partial \bar{x}}+\bar{v}\frac{\partial \bar{T}}{\partial \bar{y}}=\left[\frac{\kappa}{\rho C_p}\right]\frac{\partial^2 \bar{T}}{\partial \bar{y}^2}-\left[\frac{Q_0}{\rho C_p}\right]\left(\bar{T}-\bar{T}_\infty\right), \tag{2.4}$$

$$\gamma=\left[\mu+\frac{\kappa}{2}\right]l=\mu\left[1+\frac{K}{2}\right]l \tag{2.5}$$

where $\bar{u},\bar{v}$ represent the velocity elements in the $\bar{x},\bar{y}$ directions respectively; κ – the vortex viscosity; $\bar{N}$ – the micro-rotation; j – the microinertia density; γ – the spiral gradient viscosity; $K=\frac{\kappa}{\mu}$ – the micropolar factor and $l=\frac{\upsilon}{c}$ as the reference length.

Related boundary conditions are as follows:

$$\bar{u}=\bar{u}_w=a\bar{x}+L\frac{\partial \bar{u}}{\partial \bar{y}},\quad \bar{v}=V_0(\bar{x}),\quad \bar{N}=-n\frac{\partial \bar{u}}{\partial \bar{y}},\quad -\kappa\frac{\partial \bar{T}}{\partial \bar{y}}=h_f\left(\bar{T}_f-\bar{T}\right),\quad \text{at}\quad \bar{y}=0,$$
$$\bar{u}=\bar{u}_e(\bar{x})\to c\bar{x},\qquad \bar{N}\to 0,\qquad \bar{T}\to\bar{T}_\infty,\qquad \text{as}\quad \bar{y}\to\infty. \tag{2.6}$$

Here L is the length, $V_0(\bar{x})$ - transpiration velocity at the wall, h_f - heat transfer coefficient, $\bar{T}_f$ - fluid temperature, $n(0\le n\le 1)$ - boundary value factor. For $n=0$ *i.e.* $\bar{N}=0$ we have a non-spiral state. (The micro-components in the concentrated flow particles could not rotate near the wall) and for $n=\frac{1}{2}$ the anti-symmetric part of the stress tensor disappears and this implies a feeble concentration. Also for $n=1$ we have turbulent flows.

Introduce the following similarity variables:

$$n=\sqrt{\frac{c}{\upsilon}}\bar{y},\qquad \psi=\sqrt{c\upsilon}\,\bar{x}f(\eta),\qquad \bar{N}=c\bar{x}\sqrt{\frac{c}{\upsilon}}g(\eta),\qquad \theta(\eta)=\frac{\bar{T}-\bar{T}_\infty}{\bar{T}_f-\bar{T}} \tag{2.7}$$

Equations (2.1)-(2.4) now reduce to:

$$[1+K]f'''+ff''+1-f'^2+Kg'=0 \tag{2.8}$$

$$\left[1+\frac{K}{2}\right]g''+fg'-f'g-K(2g+f'')=0 \tag{2.9}$$

$$\theta''+\Pr f\theta'-\Pr Q\theta=0 \tag{2.10}$$

Conditions (2.6) become:

$$f(0)=F_w,\quad f'(0)=\varepsilon+\delta f''(0),\quad g(0)=-\eta f''(0),\quad \theta'(0)=-B_i(1-\theta(0)),$$
$$f'(\infty)=1,\quad g(\infty)=0,\quad \theta(\infty)=0. \tag{2.11}$$

Here $F_w = -\dfrac{V_0}{\sqrt{c\upsilon}}$ is the suction/injection factor; $\Pr = \dfrac{\mu C_p}{k}$ – Prandtl number; $Q = \dfrac{Q_0}{c\rho C_p}$ – heat source/sink; $\varepsilon = \dfrac{a}{c}$ – shrinking factor; $\delta = L\sqrt{\dfrac{c}{\upsilon}}$ – slip factor; $B_i = \dfrac{h_f}{k}\sqrt{\dfrac{\upsilon}{c}}$ – Biot number.

The physical factors, i.e., shearing stress C_f ; couple stress $M_{\bar{x}}$; Nusselt number $\mathrm{Nu}_{\bar{x}}$ are defined as:

$$C_f = \frac{\tau_w}{\rho \bar{u}_e^{\,2}}, \qquad M_{\bar{x}} = \frac{m_w}{\rho\upsilon\bar{u}_e}, \qquad \mathrm{Nu}_{\bar{x}} = \frac{\bar{x}q_w}{k(\bar{T}_\infty - \bar{T}_m)}. \tag{2.12}$$

Surface shear stress τ_w ; surface couple stress m_w ; surface heat q_w are given by

$$\tau_w = \left[(\mu+\kappa)\frac{\partial\bar{u}}{\partial\bar{y}} + \kappa N\right]_{\bar{y}=0}, \qquad m_w = \left[\left(\mu + \frac{\kappa}{2}\right) l \frac{\partial \bar{N}}{\partial \bar{y}}\right]_{\bar{y}=0}, \qquad q_w = -\left(\kappa \frac{\partial \bar{T}}{\partial \bar{y}}\right)_{\bar{y}=0}. \tag{2.13}$$

From Eqs (2.13) we get

$$\mathrm{Re}_{\bar{x}}^{\,1/2} C_f = [1+(1-n)K] f''(0), \qquad M_{\bar{x}} = \left(1 + \frac{K}{2}\right) g'(0), \qquad \mathrm{Re}_{\bar{x}}^{\,-1/2} Nu_{\bar{x}} = -\theta'(0) \tag{2.14}$$

where $\mathrm{Re}_{\bar{x}} = u_e(\bar{x})\bar{x}/\upsilon$ is the local Reynolds number.

3. Computational techniques

A shooting technique along with Runge-Kutta fourth-order method was employed to solve Eqs (2.8)-(2.10). Before, solving the nonlinear equations, first, transform these equations into a set of seven differential equations (first-order). Equation (2.11) has only four initial conditions, but it needs seven conditions to solve the set of differential equations (first-order). Thus, it is required to find three more conditions, i.e., $f''(0)$, $g'(0)$ and $\theta'(0)$ which were not present. Initially, the guesstimate values for $f''(0)$, $g'(0)$ and $\theta'(0)$ were used to solve the equations. The solution must fulfill the conditions $f''(\eta) = 1$, $g'(\eta) = 0$ and $\theta'(\eta) = 0$. i.e., In the computation process it is essential to select an appropriate finite value, say η_∞ for $\eta \to \infty$ Calculated values of $f''(\eta)$, $g'(\eta)$ and $\theta'(\eta)$ at $\eta = \infty$ are matched with $f''(\eta) = 1$, $g'(\eta) = 0$ as well as $\theta'(\eta) = 0$ at $\eta = \infty$ If it is not satisfied by calculated numerical values then the guesstimate values are revised to proceed as above to find a better solution. The procedure is continued till the desired results are obtained.

4. Results and discussion

The present outcomes of $f''(0)$ as well as $-\theta'(0)$ are compared with the outcome of Wang [2], Yacob *et al.* [17], and Khilap Sing *et al.* [20] as shown in Tab.1. The results agreed very well.

The velocity, angular velocity along with temperature for dissimilar values of F_w, K and stable values of other factors taken into consideration are computed numerically and are shown in the form of graphs in Figs 2-4. The positive values of F_w and negative values of F_w refer to suction and injection at the plate.

From Fig.2, we notice that for mass injection, the velocity of the liquid declines gradually nearby the wall $(0 \le \eta \le 1.75)$, and the reverse is seen at a distance from the plate. Whereas in the case of suction velocity

increases gradually as η increases, since suction confirms the growth of the boundary layer. Raising values of the micropolar factor K decrease the velocity. A thicker boundary layer was observed for high values of the micropolar factor. Due to an increase in the micropolar factor K, the concentration of the micro-elements near the boundary increases. The velocity of the liquid is generally high in the case of suction in comparison with injection.

Table 1. Similarity results for numerous values of ε and K $n=0.5$, $\mathrm{Pr}=1.0$, $\mathrm{B_i}=-\theta'(0)$ and $F_w=\delta=Q=0$.

ε	K	Wang [2]	Yacob *et al.* [17]		Khilap Sing *et al.* [20]		Our Result	
		$f''(0)$	$f''(0)$	$-\theta'(0)$	$f''(0)$	$-\theta'(0)$	$f''(0)$	$-\theta'(0)$
0	*0*	*1.2326*	*1.232588*	*- 0.570465*	*1.232586*	*- 0.570465*	*1.232591*	*- 0.570465*
0	*1*	*-*	*1.006404*	*- 0.544535*	*1.006405*	*- 0.5445350*	*1.006541*	*- 0.544535*
0.5	*0*	*0.71330*	*0.713295*	*- 0.692064*	*0.713294*	*- 0.692065*	*0.713475*	*- 0.692065*

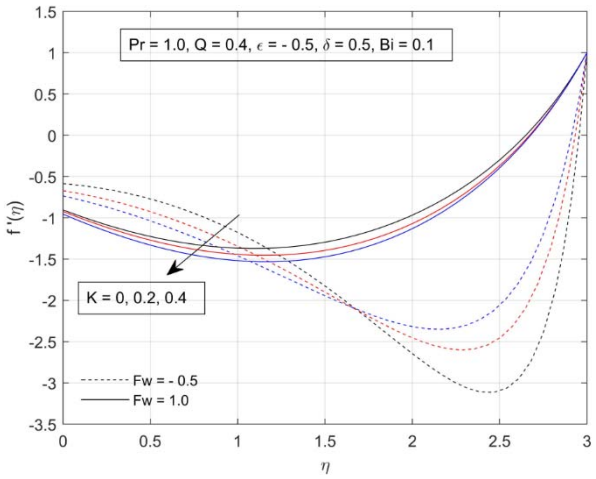

Fig.2. Result for K and F_w with $f'(\eta)$.

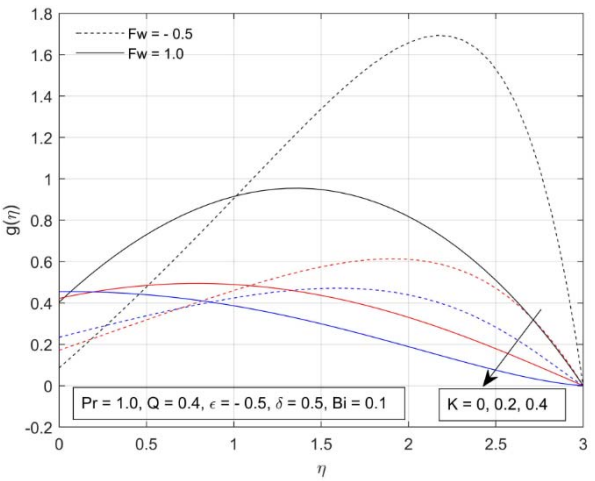

Fig.3. Result for K and F_w with $g(\eta)$.

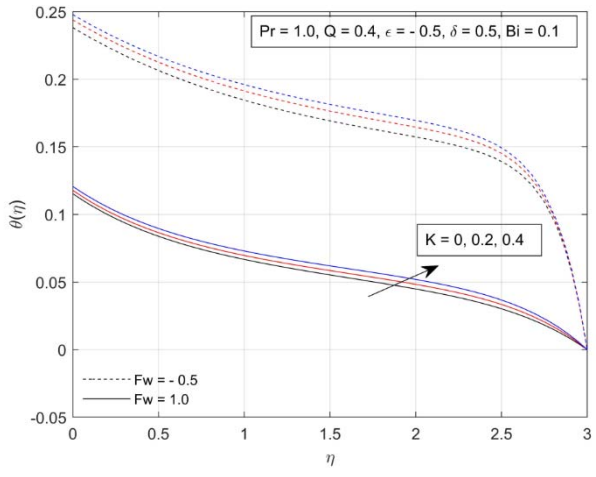

Fig.4. Result for K and F_w with $\theta(\eta)$.

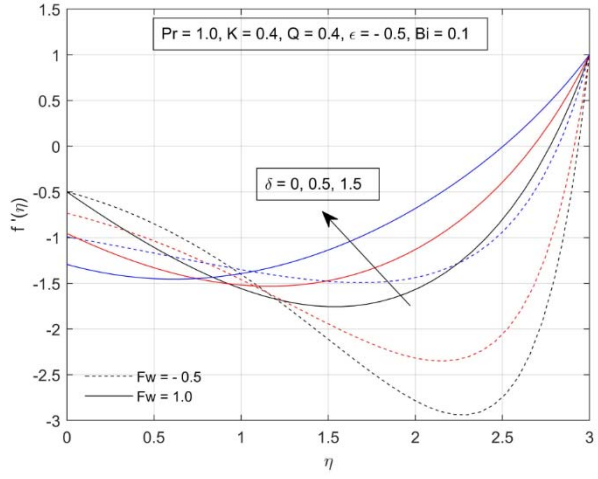

Fig.5. Result for δ and F_w with $f'(\eta)$.

In Fig.3, we see that the angular velocity of the liquid increases tremendously as η increases, subsequently it reaches its peak value at $\eta = 2.25$ and then decreases progressively as η it grows. The tendency was the same for all other values K in both cases (suction and injection). From the computed values, we noticed that the temperature of the liquid upsurges as K increases for both suction as well as injection. High values of temperature are observed in the case of injection in comparison with suction.

Figures 5-7 illustrated the impact of the slip factor δ on velocity, angular velocity, and temperatures for suction as well as injection. From Fig.5, it is clearly seen that the velocity of the liquids declines as δ upsurges and η increases nearby the plate, and the reverse is noticed at a distance from the plate irrespective of the situation (suction or injection). The angular velocity declines as δ increases which are shown in Fig.6. But the reverse trend is noticed as the temperature upsurges as δ grows as shown in Fig.7.

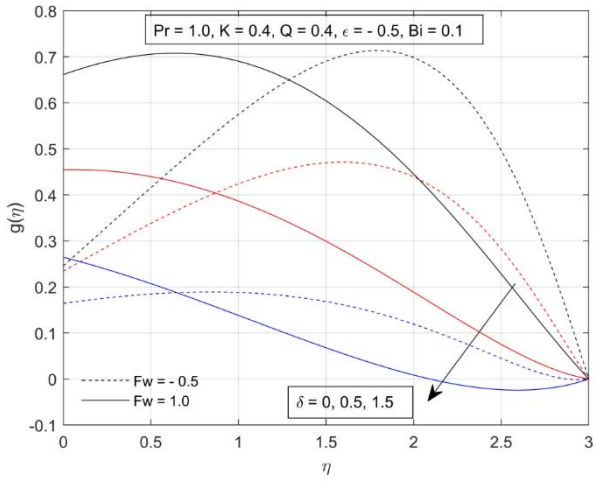

Fig.6. Result for δ and F_w with $g(\eta)$.

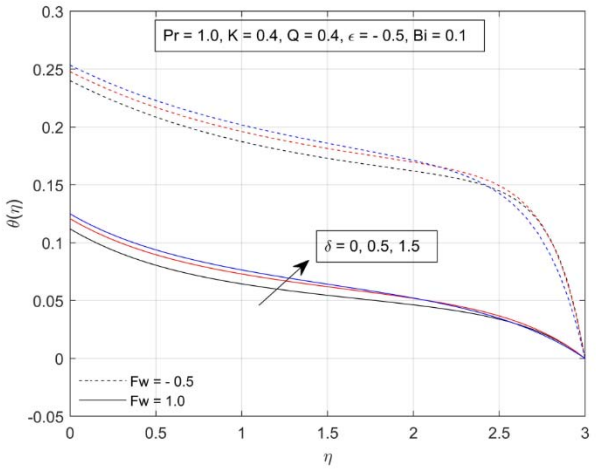

Fig.7. Result for δ and F_w with $\theta(\eta)$.

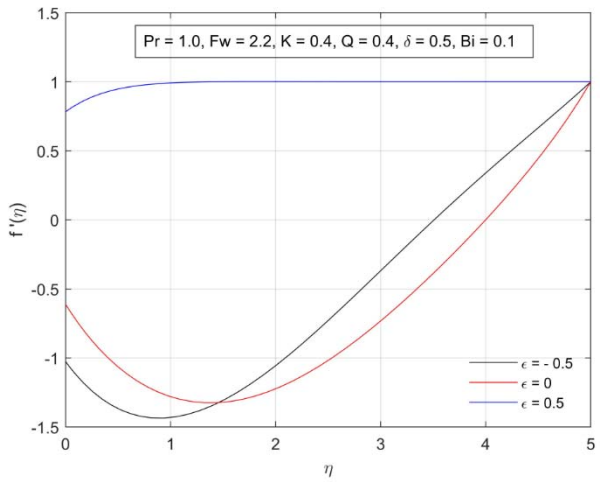

Fig.8. Result for ε with $f'(\eta)$

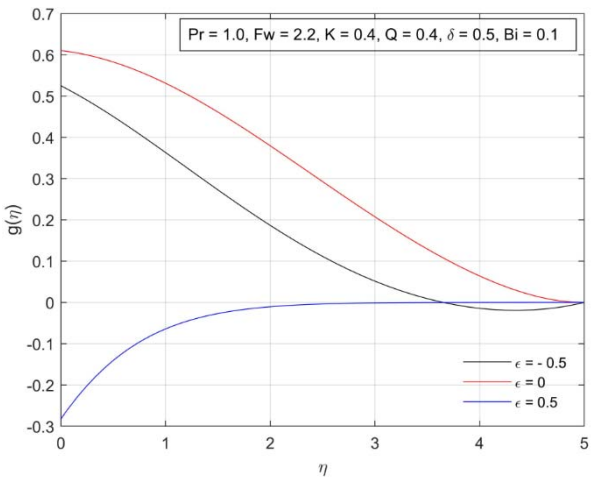

Fig.9. Result for ε with $g(\eta)$.

The influence of the shrinking parameter (ε) on velocity, angular momentum and temperature is displayed in Figs 8-10 accordingly. From Fig.8, we determined that the velocity of the liquid for ($\varepsilon = 0$) is larger nearby the plate than the velocity of the contracting sheet, but the reverse tendency is noticed at a distance from the sheet. Also, we see that the velocity of the liquid in the case of elongating sheet is larger than the case of the contracting sheet. From Fig.9, we concluded that the angular momentum is greater (for

$\varepsilon = 0$) in comparison with the contracting sheet. Also, we observed that the angular momentum is larger in the case of the contracting than the stretching sheet. From Fig.10, we see that the temperature of the liquid declines as the shrinking parameter (ε) increases.

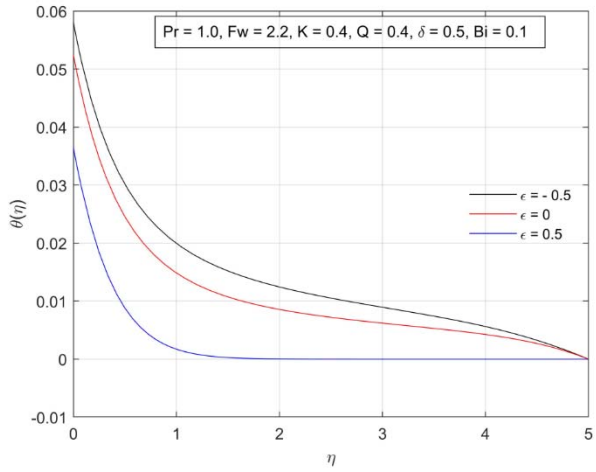

Fig.10. Result for ε with $\theta(\eta)$.

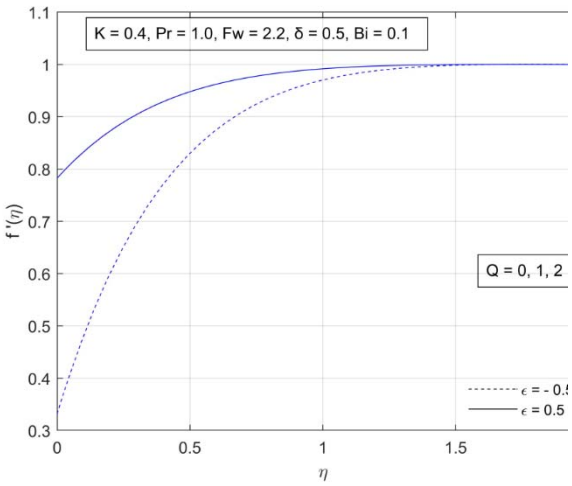

Fig.11. Result for Q and ε with $f'(\eta)$.

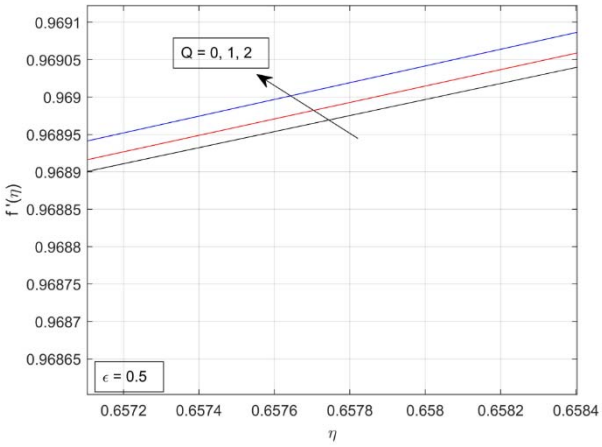

Fig.12. Details of the impact of Q and $\varepsilon = 0.5$ with $f'(\eta)$.

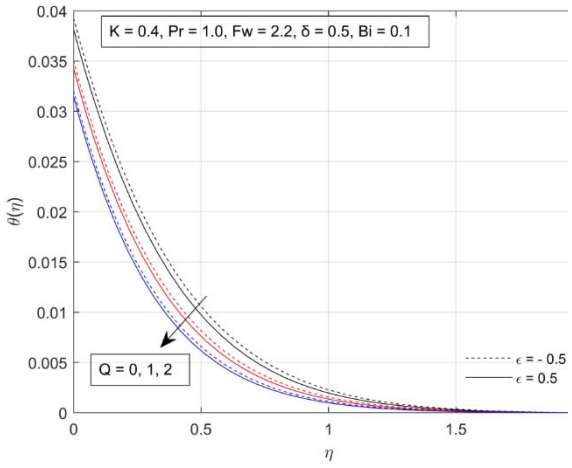

Fig.13. Result for Q and ε with $\theta(\eta)$.

The effects of the heat source factor Q and shrinking factor ε on the velocity and temperature were explained through Figs 11-13 accordingly. If there is a heat source then the liquid velocity is observed to upsurge, i.e., when heat is generated, the flow rate is intensified, which in turn upsurges the velocity profile. Also, we observed that the velocity of a micropolar fluid for the elongating sheet is higher than the values for the contracting sheet. The computed numerical values of $\theta(\eta)$ for varying values of Q and ε were obtained and shown graphically in Fig.13. We infer from this figure that the temperature of the liquid is higher for the shrinking sheet than for the stretching sheet. In case of growing values of the heat source factor Q, we noticed that the liquid temperature declines. Due to the occurrence of heat generation, the thermal boundary layer grows thicker and the liquid becomes warmer.

The analysis of varying values of Pr and Q with $f'(\eta)$ and $\theta(\eta)$ was carried out and shown in Figs 14-16 respectively. The velocity of $\Pr = 1.0$ is greater than the velocity of $\Pr = 5.0$ as shown in Figs 14 and 15.

Physically, increasing the Pr reduces the thermal diffusivity and these events lead to a decrease in the energy efficiency that diminishes the thermal boundary layer. We concluded that the velocity of the liquid increases due to upsurging value of Q. In Fig.16, it follows that the temperature of the micropolar fluid declines by the upsurging values of Pr. Also, we concluded that the temperature of the liquid decreases as Q increases.

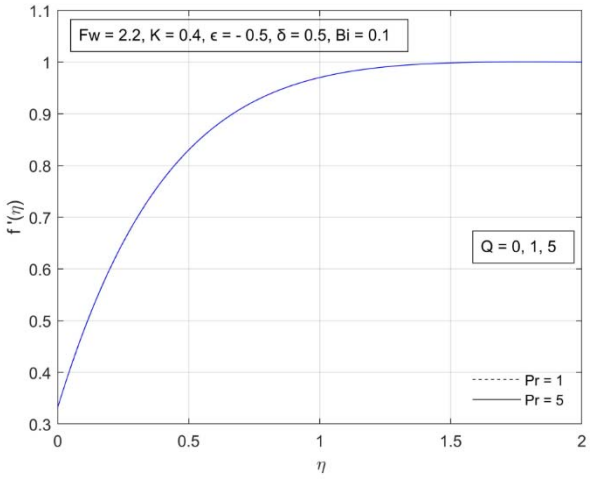

Fig.14. Result for Pr and Q with $f'(\eta)$.

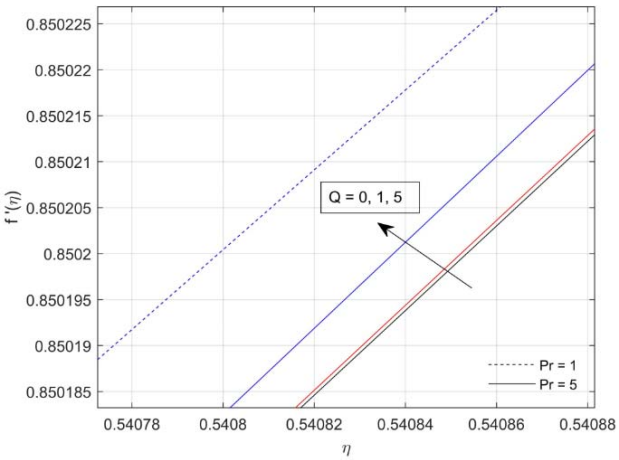

Fig.15. Details of the impact of Pr and Q with $f'(\eta)$

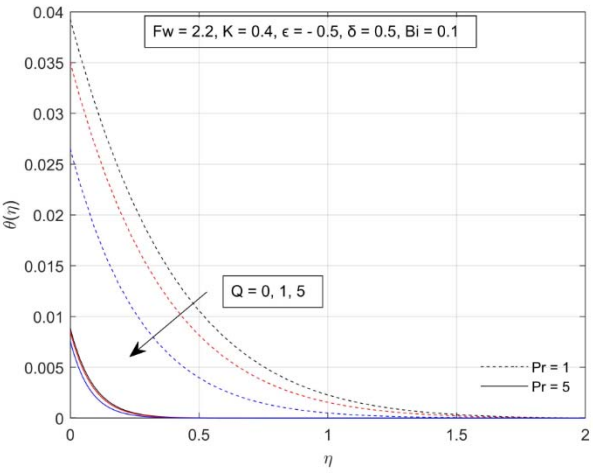

Fig.16. Result for Pr and Q with $\theta(\eta)$.

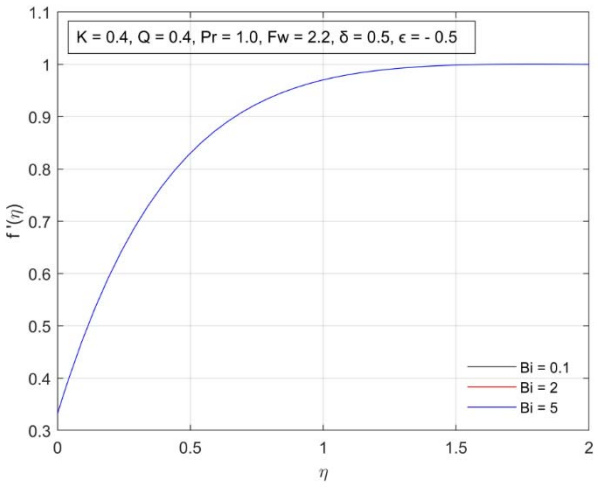

Fig.17. Result for B_i with $f'(\eta)$.

The impacts of the Biot number B_i on ($f'(\eta)$ as well as $\theta(\eta)$) were displayed in Figs 17 and 18, correspondingly. Computed values show that there is no significant effect on the velocity for varying values of B_i. The temperature grows as B_i upsurges.

Table 2 shows the effects of K, Q, B_i, ε, Pr, δ, F_w on shearing stress, heat transfer, and couple stress. The negative sign of the wall temperature flux indicates the physical reality that the heat flows from the surface to the surrounding fluid for all values of factors taken into consideration. From the numerical values, by decreasing the value of δ, the skin friction is found to grow but the reverse trend is noticed for the couple stress and heat transfer rate. Also, it is noticed that the shearing stress, couple stress and rate of heat transfer upsurges as the Biot number B_i upsurges. Growing values of the shrinking factor ε increase the shearing stress, couple stress, and Nusselt number.

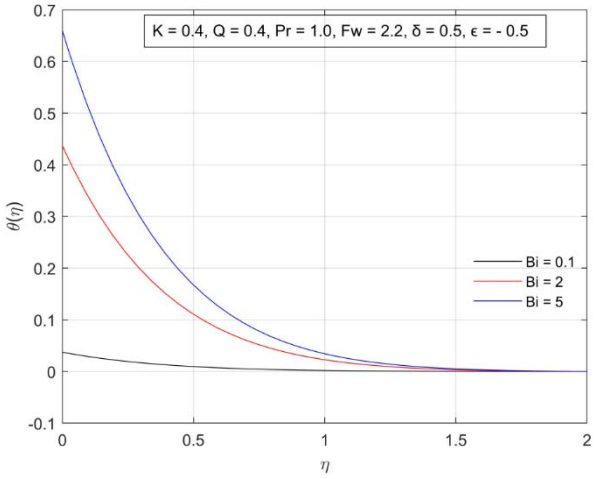

Fig.18. Result for B_i with $\theta(\eta)$.

Table 2. Variation of $f''(0), g'(0)$ and $-\theta'(0)$ for a combination of parameter values at $n = 0.5$, $\Pr = 1.0$.

K	Q	B_i	ε	Pr	δ	F_W	$f''(0)$	$g'(0)$	$-\theta'(0)$
1	*0*	*0.1*	*- 0.5*	*1*	*0.02*	*0.2*	*1.339099*	*0.347962*	*0.083879*
1	*0*	*0.1*	*- 0.5*	*1*	*0.01*	*0.2*	*1.342979*	*0.343953*	*0.083751*
1	*0*	*5*	*- 0.5*	*1*	*0.02*	*0.2*	*1.339112*	*0.347967*	*0.471284*
1	*0*	*0.1*	*- 1*	*1*	*0.02*	*0.2*	*1.303338*	*0.104529*	*0.075405*
1	*0*	*0.1*	*- 0.5*	*1*	*0.02*	*0.5*	*1.532621*	*0.515344*	*0.088129*
1	*0*	*0.1*	*- 0.5*	*5*	*0.02*	*0.2*	*1.339466*	*0.348133*	*0.091680*
1	*0.5*	*0.1*	*- 0.5*	*1*	*0.02*	*0.2*	*1.339111*	*0.347967*	*0.089520*
0.5	*0*	*0.1*	*- 0.5*	*1*	*0.02*	*0.2*	*1.479143*	*0.429814*	*0.084428*

5. Conclusion

The 2-D micropolar fluid flow along a flat linear permeable shrinking surface with slip has been investigated. The equations were converted into differential equations (ordinary) by using the suitable similarity quantities. An impact of various factors on the velocity, micro-rotation along with temperature contours was discussed elaborately.

The significant outcomes of our investigation achieved through graphical depictions are listed below:

1. We observe that for mass injection, the velocity of the liquid declines gradually nearby the wall $(0 \le \eta \le 1.75)$, and then a reverse tendency is noticed at a distance from the plate.
2. High values of temperature are observed in the case of injection as compared to the suction case.
3. The angular momentum is larger in the case of contracting than the stretching sheet.
4. Shearing stress and couple stress are reduced by increasing the value of K.

Nomenclature:

a – wall stretching factor

B_i – Biot number

c – free stream velocity factor

Cp – specific heat at constant pressure

C_f – shearing stress

f' – dimensionless fluid velocity

g' – dimensionless angular velocity

F_w – suction/injection factor

h_f – heat transfer coefficient

j – microinertia density

K – micropolar factor

l – reference length

L – length

$M_{\bar{x}}$ – couple stress

m_w – surface couple stress

n – boundary value factor

$\bar{N}$ – micro-rotation

$\mathrm{Nu}_{\bar{x}}$ – Nusselt number

Pr – Prandtl number

Q – heat source/sink factor

q_w – surface heat flux

$\mathrm{Re}_{\bar{x}}$ – local Reynolds number

$\bar{T}_f$ – fluid temperature

$\bar{T}_\infty$ – free stream temperature

$\bar{u}$ – velocity along the surface

$\bar{u}_e$ – free stream velocity

$\bar{v}$ – velocity perpendicular to the surface

$V_0(\bar{x})$ – transpiration velocity

$\bar{x}$ – direction along the surface

$\bar{y}$ – direction perpendicular to the surface

γ – spiral gradient

δ – slip factor

ε – shrinking factor

η – boundary layer length

θ – dimensionless temperature

υ – kinematic viscosity

κ – vortex viscosity

μ – dynamic viscosity

ρ – fluid density

τ_w – surface shear stress

References

[1] Miklavčič M. and Wang C.Y. (2006): *Viscous flow due to a shrinking sheet*.– Q. Appl. Math., vol.64, pp.283-290.

[2] Wang C. Y. (2008): *Stagnation flow towards a shrinking sheet*.– Int. J. Nonlinear Mech., vol.43, pp.377-382.

[3] Nadeem S., Hussain A., Malik M. Y. and Hayat T. (2009): *Series solutions for the stagnation flow of a second-grade fluid over a shrinking* sheet.– Appl. Math. Mech., vol.30, pp.1255-1262.

[4] Bachok N., Ishak A, and Pop I. (2010): *Melting heat transfer in boundary layer stagnation-point flow towards a stretching/shrinking sheet*.– Phy. Lett. A, vol.374, pp.4075-4079.

[5] Fan T., Xu H, and Pop I. (2010): *Unsteady stagnation flow and heat transfer towards a shrinking sheet*.– Int. Comm. Heat Mass Tran., vol.37, pp.1440-1446.

[6] Rosali H., Ishak A. and Pop I. (2011): *Stagnation point flow and heat transfer over a stretching/shrinking sheet in a porous medium*.– Int. Comm. Heat and Mass Tran., vol.38, pp.1029-1032.

[7] Bhattacharyya K. and Vajravelu K. (2010): *Stagnation-point flow and heat transfer over an exponentially shrinking sheet*.– Comm. Nonlinear Sci. Numer. Simul., vol.17, pp.2728-2734.

[8] Bachok N., Ishak A. and Pop I. (2013): *Boundary layer stagnation-point flow toward a stretching/shrinking sheet in a nanofluid*.– ASME J Heat Tran., vol.135, p.5. https://doi.org/10.1115/1.4023303

[9] Eringen A. C. (1966): *Theory of micropolar fluids*.– J. Math. Mech., vol.16, pp.1-18.

[10] Kumari M. and Nath G. (1984): *Unsteady incompressible boundary layer flow of a micropolar fluid at a stagnation point*.– Int. J Eng. Sci., vol.22, pp.755-768.

[11] Ziaul Haque Md., Mahmud Alam Md., Ferdows M. and Postelnicu A.: *Micropolar fluid behaviors on steady MHD free convection and mass transfer flow with constant heat and mass fluxes, Joule heating, and viscous dissipation*.– Journal of Kind Saud University Engineering Sciences, vol.24, pp.71-84.

[12] Uddin Z. and Kumar M. (2013): *Hall and ion-slip effect on MHD boundary layer flow of a micropolar fluid past a wedge*.– Scientia Iranica B, vol.20, No.3, pp.467-476.

[13] Borrelli A., Giantesio G. and Patria M. C. (2015): *An exact solution for the 3D MHD stagnation point flow of a micropolar fluid*.– Commun Nonlinear Science and Numerical Simulation, vol.20, pp.121-135.

[14] Siva Reddy Sheri and Shamshuddin MD. (2015): *Heat and mass transfer on the MHD flow of micropolar fluid in the presence of viscous dissipation and chemical reaction*.– Procedia Engineering, vol.127, pp.885-892.

[15] Rahman M. M., Rahman M. A., Samad M. A. and Alam M. S. (2009): *Heat transfer in a micropolar fluid along with a non-linear stretching sheet with temperature-dependent viscosity and variable surface temperature*.– Int. J Thermophys., vol.30, pp.1649-1670.

[16] Ishak A., Lok Y. Y. and Pop I. (2010): *Stagnation-point flow over a shrinking sheet in a micropolar fluid*.– Chem. Eng. Comm., vol.197, pp.1417-1427.

[17] Yacob N. A., Ishak A. and Pop I. (2011): *Melting heat transfer in boundary layer stagnation point flow towards a stretching/shrinking in a micropolar fluid*.– Computers & Fluids, vol.47, pp.16-21.

[18] Bhattacharyya K., Mukhopadhyay S., Layek G. C. and Pop I. (2012): *Effects of thermal radiation on micropolar fluid flow and heat transfer over a porous shrinking sheet*.– Int. Journal of Heat and Mass Transfer, vol.55, pp.2945-2952.

[19] Hussain M., Ashraf M., Nadeem S. and Khan M. (2013): *Radiation effects on the thermal boundary layer flow of a micropolar fluid towards a permeable stretching sheet*.– Journal of The Franklin Institute, vol.350, pp.194-210.

[20] Khilap Singh, Pandey A. K., and Manoj Kumar. (2019): *Analytical approach to stagnation point flow and heat transfer of a micropolar fluid via a permeable shrinking with slip and convective boundary conditions*.– Heat Transfer Research, vol.50, No.8, pp.739-756.

[21] Subhas Abel M., Datti P. S. and Mahesha N. (2009): *Flow and heat transfer in a power-law fluid over a stretching sheet with variable thermal conductivity and non-uniform heat source*.– Int. Journal of Heat and Mass Transfer., vol.52, pp.2902-2913.

[22] Mahmoud M. A. A. and Waheed S. E. (2012): *MHD flow and heat transfer of a micropolar fluid over a stretching surface with heat generation(absorption) and slip velocity*.– Journal of the Egyptian Mathematical Society, vol.20, pp.20-27.

[23] Mabood F., Ibrahim S.M., Rashidi M. M., Shadloo M. S. and Lorenzini G. (2019): *Nonuniform heat source/sink and Soret effects on MHD non-Darcian convective flow past a stretching sheet in a micropolar fluid with radiation*.– Int. Journal of Heat and Mass Transfer, vol.92, pp.674-682.

[24] Muthamilselvan M., Periyadurai K. and Doh D. H. (2017): *Effect of uniform and nonuniform heat source on natural convection flow of micropolar fluid*.– Int. J of Heat and Mass Tran., vol.115, pp.19-34.

[25] Mishra S. R., Hoque M. M., Mohanty B. and Anika N. N. (2019): *Heat transfer effect on MHD flow of a micropolar fluid through porous medium with uniform heat source and radiation*.– Nonlinear Engineering, vol.8, pp.65-73.

Received: October 2, 2020
Revised: February 17, 2021